A STUDY OF FAILURE ASSESSMENT DIAGRAM (FAD) UNDER BIAXIAL LOADING

Dong-Ming Tan, Weng-Long Huang, Shu-Ho Dai
Nanjing Institute of Chemical Technology
Nanjing, Jiangsu, 210009, People's Republic of China

Third International Conference on Biaxial/Multiaxal Fatigue, April 3-6, 1989 Stuttgart, FRG

ABSTRACT

A fracture experiment under biaxial loading and theoretical analysis has been used to study the fracture behaviour of cruciform specimen, made of a Chinese Industrial Standard steel 16MnR, with a centre penetrated crack and the Failure Assessment Diagram (FAD) for evaluating the safety margin of cracked structure under biaxial loading is explorated. The fracture parameters J-integral based on elastic, Je, and elastic-plastic, Jep are calculated by finit element method and the instantaneous load of initiation of crack growth is examined by the method of local D.C. electric potential measurement. Upon the research work mentioned above, the modified methods of failure assessment of CEGB [1] R6 and EPRI [2] Engineering Approach for biaxial loading have been proposed respectively in the present work. The experiment results reveal that the J-integrals based on the measured instantanous load of initiation of crack growth, Ji, under different ratio of biaxial load are, in general, almost identically equal, however, the JR curve of J-integral based on the contralling condition of crack propagation is affected by different ratio of biaxial load. In comparsion, it is found that the modified Failure Assessment Diagram of EPRI method for the biaxial loading proposed is more agreed with the experiment result than the others.

KEY WORDS: fracture, biaxial, cruciform, Failure Assesment Diagram, J-integral, J-resistance curve

1. INTRODUCTION

In recent year several proposals have been developed which are aimed at assessing the safety of the nuclear and chemical industries structures which might fail by ductile mechanism. The CEGB's R6 and the EPRI's JFAD are the important methods of failure assessment. Biaxial and multiaxial stress states are common in pressure vessels and piping. A large number

of investigation of failure assesment are based on uniaxial stress states. Experiments are carried out in uniaxial specimens such as CS, CCP, SECP, DECP. When the results of the investigations are used in engineering, some questions will be raised, e.g. whether the results in uniaxial stress states are completely available to the biaxial and multiaxial stress states in engineering, whether they are conservative or not, how much the errors are. To attempt answer these questions, the fracture experiments in biaxial stress states are carried out in present work. The centre cracked cruciform specimens are made of a Chinese Industrial Standard steel 16MnR for pressure vessels. Based on the result of the numerical and theoretical analysis, the modified methods of failure assessment of CEGB's R6 and EPRI's JFAD for biaxial loading have been proposed respectively in the present work.

2. BRIEF INTRODUCTION OF FAILURE ASSESSMENT METHODS

The CEGB R6 failure Assessment Method

The CEGB failure assesment diagram uses the non- dimensional load and stress intensity parameters Kr and Sr defined by

$$Kr=K/Kc=(K^2/EJc)^{\frac{1}{2}} \tag{1}$$

$$Sr=P/P_L(\sigma) \tag{2}$$

where Kc is the material tonghness and PL($\overline{\sigma}$) the limit load defined for yield or flow stress $\overline{\sigma}$. For a centain structure, given loadings and defect sizes, the two parameters Kr and Sr are evaluated from EQ.1 and EQ.2, if assessment point (Sr,Kr) lies within the failure assessment curve, the defect is acceptable. The assessment curve is

$$Kr^2=Sr^2\sqrt{[\frac{8}{\pi^2}\ln\sec(\frac{\pi}{2}Sr)]} \tag{3}$$

Milne [3] modified the assessment curve in consideration of strain hardening as

$$Sr=\sigma/\sigma_o+(1-Kr^{\frac{1}{2}})(\sigma_u/\sigma_0-1) \tag{4}$$

where σ_u is the ultimate stress and σ_y the yield stress.

EPRI Failure Assessment Diagram

Bloom [4] devived JFAD using the J estimation scheme proposed by Kumar The stress-strain curve may be described by

$$\epsilon/\epsilon_o=\sigma/\sigma_o+\alpha(\sigma/\sigma_o)^n \tag{5}$$

For a material obeying EQ.5, Kumar suggested the value of J

$$J=K^2(a_e)/E'+\alpha\sigma_0\epsilon_0Ch(a/w,n)(P/P_0)^{n+1} \tag{6}$$

The J-contralling condition for stable growth

$$J_{ep}(a,P)=J_R(a) \tag{7}$$

can be written as

$$J(a_e)(P/P_0)^2+J(a,n)(P/P_0)^{n+1}=J_R(\Delta a) \tag{8}$$

The normalized coordinatates are defined by

$$Kr^2=Je/J_R \qquad Sr=P/P_0 \tag{9}$$

Failure assessment curve can be devived

$$Kr^2=Sr^2/(HeSr^2+HnSr^{n+1})=f(Sr) \tag{10}$$

where $He=J(a_e)/J(a)$ $Hn=J(a,n)/J(a)$

3.EXPERIMENT

Material Properties

The specimens were machined to a thickness of 5 mm, made of a Chinese Industrial Standard steel 16MnR. The mechnical properties and composition of 16MnR steel are given in Table 1.

Table 1. Mechanical properties and composition of 16MnR steel

Material	Mechanical Properties						Composition %				
	σ_s	σ_u	ψ	δ	E	ν					
16MnR	MPa	MPa	%	%	MPa		C	Si	Mn	P	S
	384.5	564.	57.	28.	2.05E5	0.28	0.14	0.47	1.46	0.01	0.17

Several Ramberg-Osgood fits were made to the true stress-strain data. One fits the whole stress-strain range (1). The others (2,3,4,5,6) pass the points $(\sigma_s,\epsilon_s),(\sigma_{0.2},\epsilon_{0.2}),(\sigma_u,\epsilon_u)$ respectively. R-O law is proposed as EQ.5. These fits are shown in Fig.1, and corresponding R-O coefficients are tabulated in Table 2.

Table 2. Ramberg-Osgood Coefficients

Methods	1	2	3	4	5	6
α	5.017	8.760	5.004	1.040	1.000	1.040
n	5.569	3.876	5.260	10.90	11.17	9.260

Geometry and Dimensions of the Biaxial Specimen

According to the cruciform specimen developed by K.J. Miller [5] and the present results of FEM analysis and the test machine in our lab, new specimen was redesigned. See Fig.3

The specimen were equiped with strain gages. Strain data were obtained for two crack sizes at biaxiality ratio k=0,0.5,1. (k=Px/Py). The edge-stress distribution was non-uniform due to the present of the crack, but it was in good agreement with the stress distrbution assuming uniform dis-

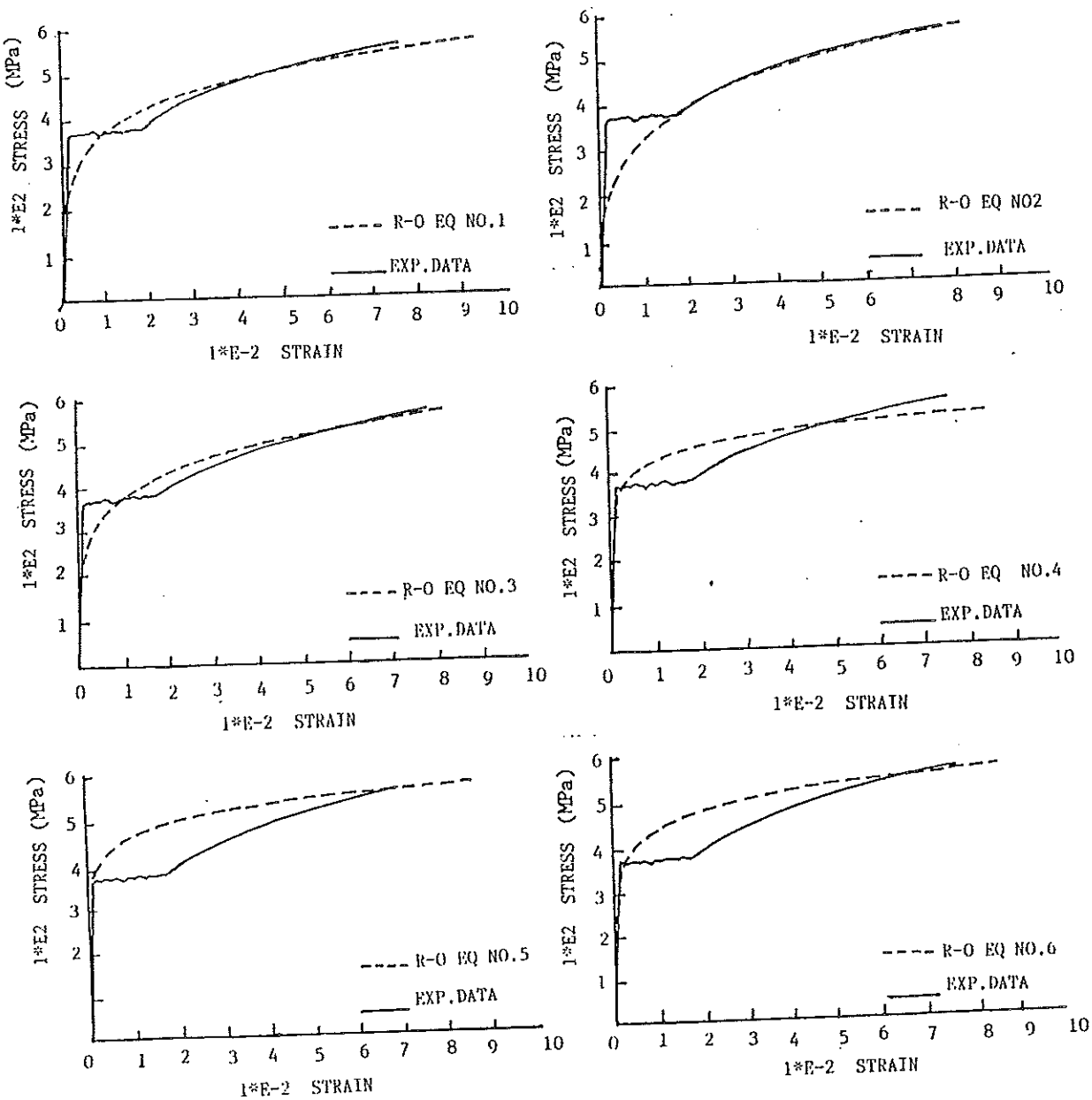

FIG 1. Ramberg-Osgood fit to a stress-strain curve for 16MnR steel at room temperature.

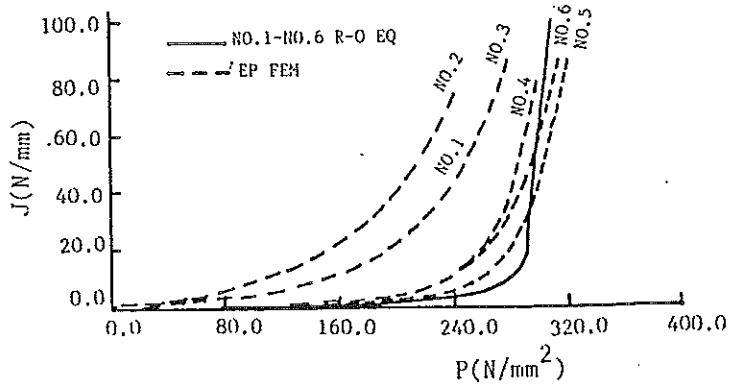

FIG 2.Comparison of the estimation method and finite element

placement of the edge. The corresponding edge and centre uniform stresses have following relations.

$$\sigma_x = 2(1.084\sigma_{xe} - 0.1275\sigma_{ye}) \quad (11)$$

$$\sigma_y = 2(1.084\sigma_{ye} - 0.1275\sigma_{ye}) \quad (12)$$

The thickness of the centre (working) part is 5 mm, and the clamping part is 10 mm.

Fracture Experiments Under Biaxial Loading

Fracture experiments were undertaken with centre penetrated crack cruciform specimen. The total crack lengths ranged from 30 mm to 55 mm, including length of spark machined notch and fatigue crack. Experiments were performed under load biaxaility ratio k=0,0.5,1 to investigate the effect of biaxial ratio on the initiation and growth of the crack.

a. Testing of crack initiation load

The thickness 5 mm will not reach the plane strain thickness12.5 mm. Local D.C. potential measurement method was used to detect the initiation. The initiation loads are tabulated in Table 3.

Table 3. Initiation load using local D.C. potential method

Specimen No.	k	a_{x1}(mm)	a_{x2}(mm)	a(mm)	Pi(T)	Pipr(T)	Error%
A13	0	18.08	18.01	18.55	20.50	19.35	5.9
A14	0	16.30	16.98	17.14	20.63	19.35	6.3
A1	0.5	17.25	17.33	17.79	21.50	23.71	9.3
A3	0.5	16.90	17.02	17.46	23.38	23.71	1.39
A5	0.5	16.85	17.01	17.46	22.75	23.71	4.04
A12	1	17.00	16.89	17.45	24.35	24.06	0.79
B5	0	21.97	22.03	22.50	16.15	16.89	2.30
B1	0.5	21.69	22.08	22.35	20.63	20.45	0.88
B3	0.5	22.07	21.75	22.41	20.88	20.45	1.22
B2	1	22.22	22.07	22.15	21.55	21.14	0.52
B4	1	21.26	21.93	22.30	20.75	21.14	1.84
C5	0	27.64	27.21	27.93	16.75	15.07	11.10
C3	0.5	25.98	26.01	26.53	17.50	17.45	0.28
C6	0.5	26.92	27.13	27.53	18.00	17.45	3.15
C7	0.5	27.42	27.57	28.00	17.63	17.45	1,03
c8	0.5	26.80	27.01	27.41	17.60	17.45	0.86
C4	1	27.32	26.80	27.56	19.38	19.06	1.68

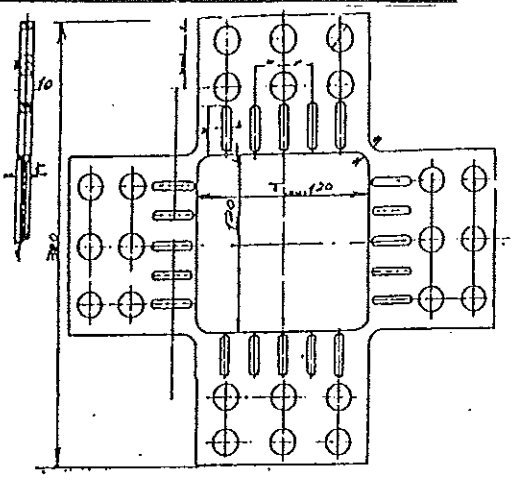

FIG 3. Biaxial Specimen

By comparing these results with the data of multi-section method, it is found that the intiation loads are in good agreement with each other, maxiam error is 3.15 %, see Table 4. It shows the reliability of the local D.C. potential method.

Table.4 Comparion of the data with potential and multi-section methods

Specimen No.	C3	C6	C7	C8	C9
Pi (T)	17.5	18.0	17.63	17.60	17.75
Error %	0.268	3.15	1.00	0.86	1.79

b. J_R curve

According to experimental P-a curves, J_R curves are devived by elastic-plastic FEM. Equations of J_R curves are obtained for different biaxial ratio by the regression of following expression:

$$J_R = A \Delta a^B \tag{13}$$

The values of A,B are given in Table 5.

Table 5. Fit coefficients of J_R curve

k	0			0.5			1		
a	30.	40.	50.	30.	40.	50.	30.	40.	50.
A	848.	1545.	1785.	85.9	346.	346.	213.	102.	140.
B	0.49	0.56	0.76	0.22	0.35	0.49	0.18	0.32	0.31
R	0.98	0.99	0.98	0.99	0.98	0.99	0.96	0.96	0.99

The J_R data distribute in Fig.4

Fig.4 Distribution of experimental data for J_R curve

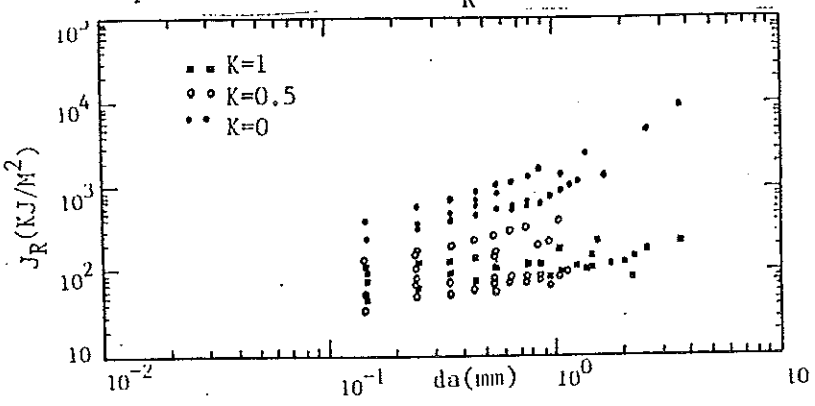

FIG 4. Distribution of experimented data for J_R-curve

The experimental results reveal that J_R curves are related with not only the original crack length but also the biaxial ratio. Uniaxial J_R curves (k=0) are higher than biaxial J_R curves (k=0.5,1). When the J_R curves are plotted in the diagram of J-integral crack driving force calculated by elastic-plastic FEM, the instability prediction will be obtained. see Fig.5.

4. FAILURE ASSESSMENT DIAGRAM IN BIAXIAL STRESS STATES

CEGB's R6 Method in Biaxial Stress States

Adam [6] proposed on extensive model(see Fig.6) to analyse the influence

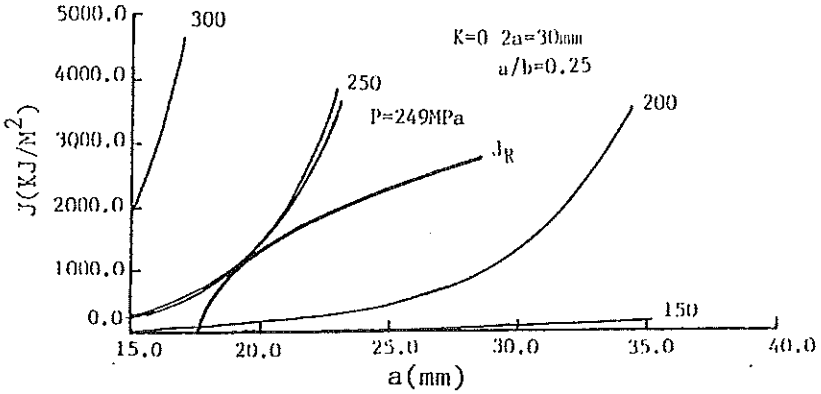

FIG 5a. Crack driving force diagram for an center-cracked cruciform flat specimen of 16MnR steel under ratio of biaxial load K=0

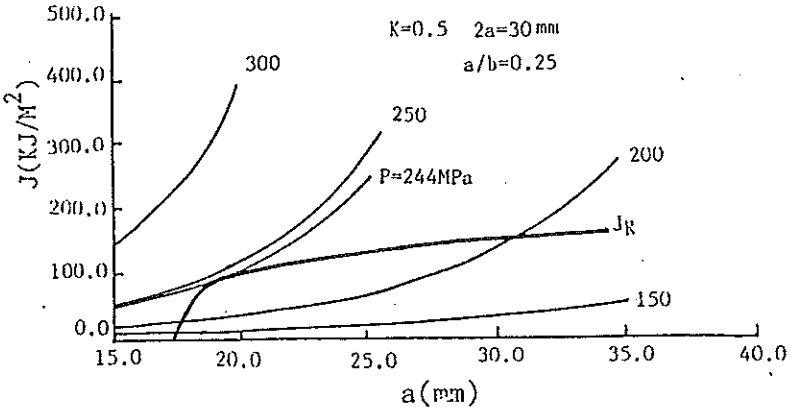

FIG 5b.Crack driving force diagram for an center-cracked cruciform flat specimen of 16MnR steel under ratio of biaxial load K=0.5.

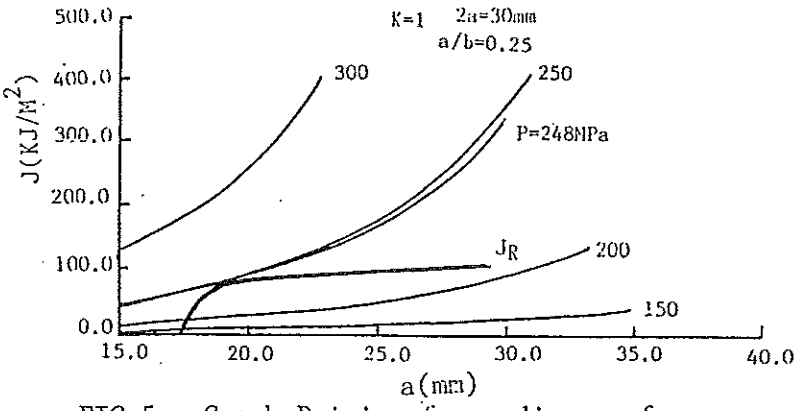

FIG 5c. Crack Driving force diagram for an center-cracked cruciform flat specimen of 16MnR steel under ratio of biaxial load K=1

of biaxial loading, and took into account of biaxial effect, and modified the restraining stress of Dugdale's model, by including the stress parallel to the crack plane as follow.

$$\delta=8\sigma^{*}a/\pi E \ln\sec\left(\frac{\pi\sigma^{\infty}}{2\sigma^{*}}\right) \tag{14}$$

$$\sigma_y=\sigma^{*}-\sigma_y+\sigma_x \tag{15}$$

$$\sigma_y=\sigma^{*} \tag{16}$$

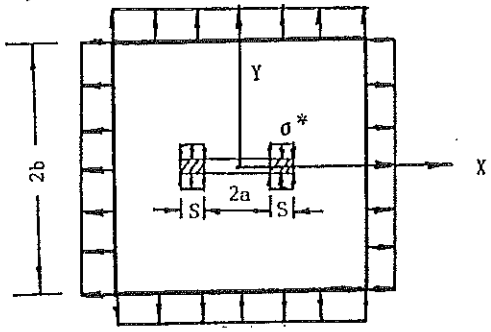

FIG 6. Modified Dugdale model.

where E is Young's modulus, σ^{*} is the restraining stress.

For Von Mises criterion

$$\sigma^{*}=\tfrac{1}{2}[(\sigma_y^{\infty}-\sigma_x^{\infty})+\sqrt{4\sigma_0^{2}-3(\sigma_y^{\infty}-\sigma_x^{\infty})^{2}}] \tag{17}$$

where σ_0 is uniaxial yield stress. By substituting σ^{*} into EQ.14, δ expresion can be obtained for infinit plate.

For a square centre-cracked thin plate, it is considered that σ^{∞}_x σ^{∞}_y in the extensive Dugdale's model can be replaced by the average stress in the net section area, and have such relations with edge distributed stresses, as follows.

$$\sigma_x=\sigma_x^{\infty}\ ,\ \sigma_y=\sigma_y^{\infty}c/b \tag{18}$$

Substituting into EQ.17, σ^{*} in square thin plate gives

$$\sigma^{*}=\tfrac{1}{2}[(\sigma_y b/c-\sigma_x)+\sqrt{4\sigma_0^{2}-3(\sigma_y b/c-\sigma_x)^{2}}] \tag{19}$$

Therefore, δ of square thin plate can be obtained.

b. Biaxially Modification of CEGB's R6

By comparing the modified R6 curve and test data assessment points, it is found that biaxially modified R6 curve gives a conservative prediction. See Fig.7.

By biaxially modifying, Milne's assessment curve can be written as

$$Kr=\sigma/\sigma^{*}\left[\frac{8}{\pi^{2}}\ln\sec\left(\frac{\pi\sigma}{2\sigma^{*}}\right)\right]^{\frac{1}{2}}$$

$$Sr=\sigma/\sigma^{*}+(1-Kr^{\frac{1}{2}})(\sigma_u/\sigma^{*}-1) \tag{20}$$

It is in good agreement with experimental results for biaxial stress states, as shown in Fig.8.

EPRI's JFAD in Biaxial Stress States

a. Fully Plastic Analysis of Crack in Biaxial Stress States

M.Y.He[7] suggests that modified principle of complementry potential energy can be used to generate upper and lower bounds to J-integral. For a crack infinite bodies. See Fig.9. For plane stress conditions, J-integral

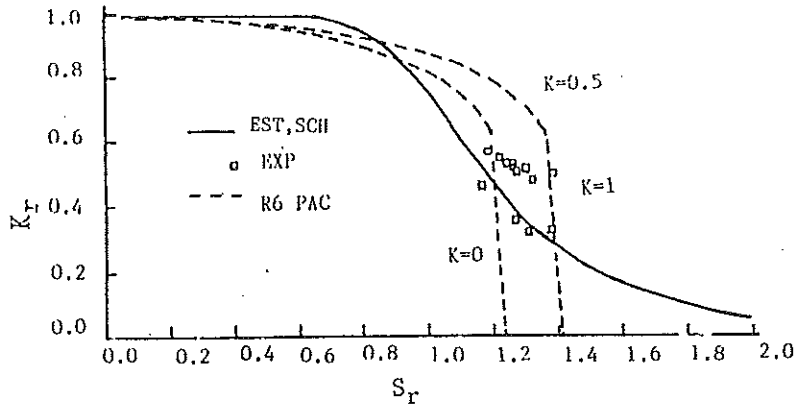

FIG 7. Comparison of the modified R6 method and experimented results

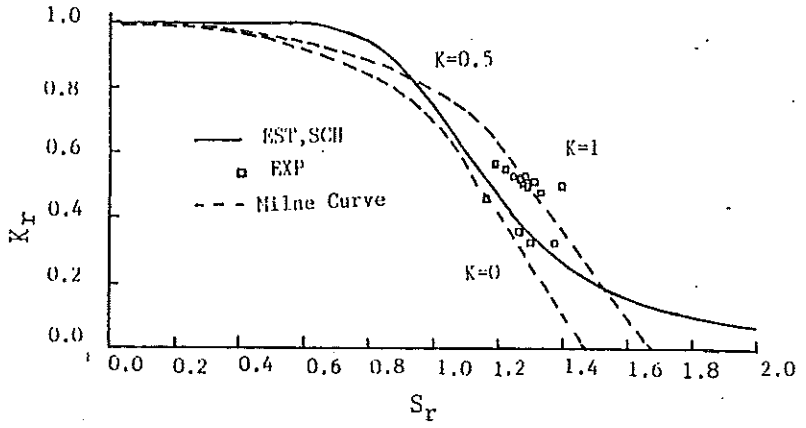

FIG 8. Comparison of the modified Milne's curve and experimented results

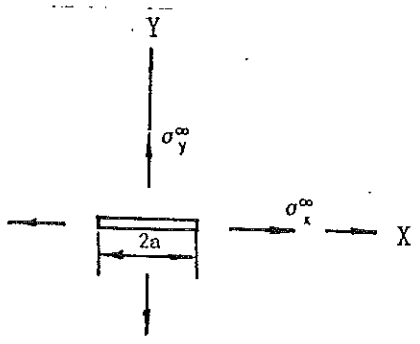

FIG 9. Infinite plate with acentral penetrated crack.

is $J = a\sigma_c^{\infty} \epsilon_e^{\infty} h(n)$

Considering a material for which the uniaxial stress strain($\sigma - \epsilon$)curve may be discribed by $\epsilon/\epsilon_0 = \alpha(\sigma/\sigma_0)^n$ (21)

The tensile relation is generalized to multi-axial states J_2 deformation theory according to $\epsilon_{ij}/\epsilon_0 = 3/2\ \alpha(\sigma_e/\sigma_0)^{n-1} S_{ij}/\sigma_0$ (22)

where S_{ij} is the stress deviator, is the efficient stress defined by

$$\sigma_e = (3/2 S_{ij} S_{ij})^{\frac{1}{2}} \quad (23)$$

With an efficient strain defined by

$$\epsilon e = (2/3\ \epsilon_{ij}\ \epsilon_{ij})^{\frac{1}{2}} \quad (24)$$

The values of h(n) are tabulated in Table 6.

Table6. Value of h(n)

n	1.0	1.5	2.0	3.0	4.0	5.0	7.0
h(n)	3.19	3.91	4.56	5.73	6.77	7.75	9.56

For plane streess states $\sigma_e^{\infty} = \sqrt{\frac{1}{2}[(\sigma_x^{\infty} - \sigma_y^{\infty})^2 + \sigma_x^{\infty 2} + \sigma_y^{\infty 2}]}$ (25)

$$\epsilon_e^{\infty} = \alpha \epsilon_0 (\sigma_e^{\infty}/\sigma_0)^n \quad (26)$$

$$J = \alpha \sigma_0 \epsilon_0 a h(n) (\sigma_e^{\infty}/\sigma_0)^{n+1} \quad (27)$$

When n=1, $J = J_e = \alpha \sigma_0 \epsilon_0 a h(1) (\sigma_e^{\infty}/\sigma_0)^2$ (28)

For square plate, it is considered that the biaxial effect on J-integral is, in general, conservative. The values of h almost remain constant when when k is changed from -1 to 1, thus J-integral is as follows,

$$J = \alpha\ \sigma_0 \epsilon_0 a h1(a/b,n) (\sigma_e/\sigma_0)^{n+1} \quad (29)$$

where h1(a/b,n) is the function of crack length and hardening constant. The values of h1 have been tabulated in Ref.2. Efficient stress is

$$\sigma_e = \sqrt{\frac{1}{2}[(\sigma_y b/c - \sigma_x)^2 + (\sigma_y b/c)^2 + \sigma_x]} \quad (30)$$

b. JFAD of Centre Cracked Cruciform Specimen under Biaxial Loading

Upon the discussion above, J_{ep} can be written as

$$J_{ep} = J_e + J_p = \alpha \sigma_0 \epsilon_0 a h(a/b,1) (\sigma_e/\epsilon_0)^2 + \alpha \sigma_0 \epsilon_0 a h1(a/b,n) (\sigma_e/\sigma_0)^{n+1} \quad (31)$$

Biaxial modified JFAD can be written as

$$Kr = [J_e/J_R(\Delta a)]^{\frac{1}{2}} = f(Sr) \quad (32)$$

where $Sr = \sigma/\sigma_0$, σ_0 is biaxial modified limit distributed stress which can be derived from limit load.

For centre cracked square thin plate, limit load P_0 can be derived by using the principle of energy equilibrium in plasiticity theory. See Fig.10.

$$P_0 = 2Ac\tau_0 \quad (33)$$

where A is biaxial coefficient.

$$A = b/(b-kc) \quad (34)$$

$$\tau_0 = \frac{1}{2}(\sigma_1 + \sigma_2) \quad (35)$$

Biaxially modified failure assessment curves can be plotted for different crack lengths and biaxiality ratios respectively,shown in Fig. 10-16. By comparing these assessment curves with experimental results give a good

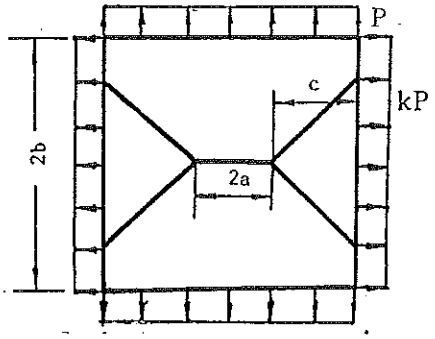

Fig.10 Limit load of square thin plate

agreement with the assessment results for different biaxiality ratios and crack lengths. The FEM results give good agreements only in the range of the experimental results. Errors appear in other range. The main reason is that 16MnR steel has a long yield platform. The Ramberg-Osgood fitting method are choosen to mininize the errors between J-integrals calculated by EQ.31 and by FEM only near the crack initiation point J_i. The other reason is that biaxiality effect on hl isneglected.

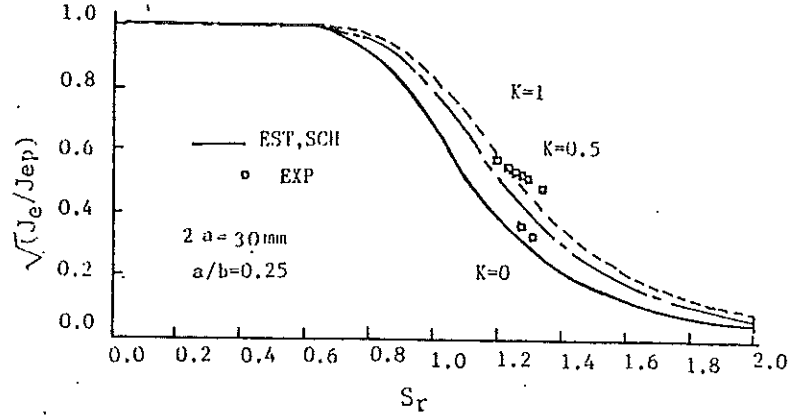

FIG 11. Comparison of the modified JFAD and experimented results.

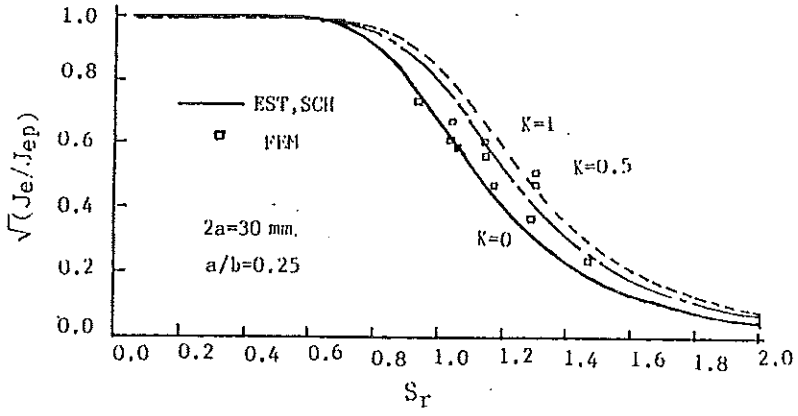

FIG 12. Comparison of the modified JFAD and Elastic-plastic finite element results.

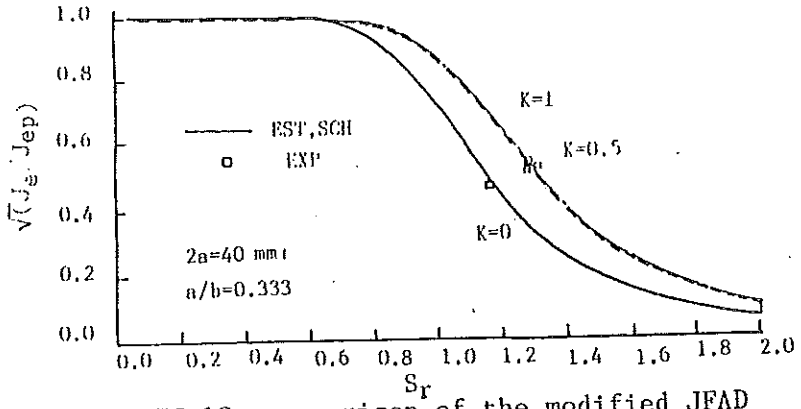

FIG 13. comparison of the modified JFAD and experimented results.

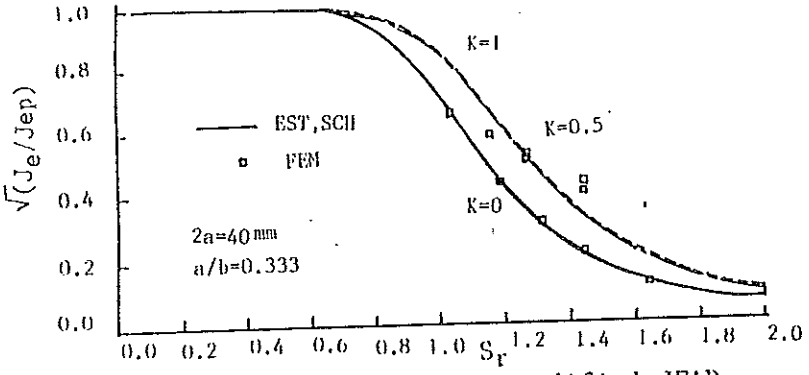

FIG 14. Comparison of the modified JFAD and Elastic-Plastic finite element results

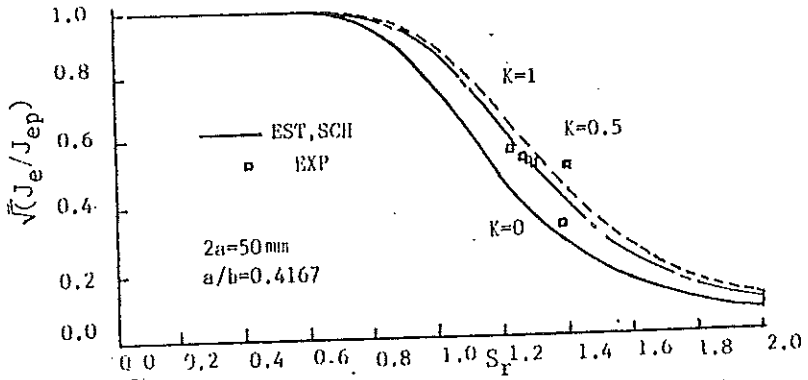

FIG 15. Comparison of the modified JFAD experimented results.

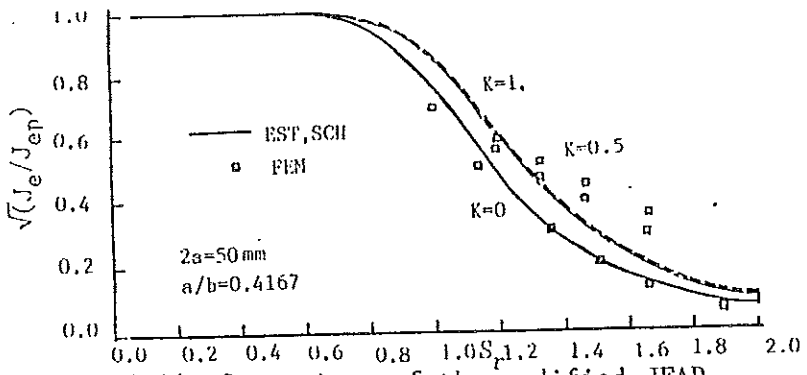

FIG 16. Comparison of the modified JFAD and Elastic-plastic finite element results

5.CONCLUSIONS

a. Experimental results reveal that the J-integrals based on the measured instantaneous load of initiation of crack growth, J_i, under different ratio of biaxial load and crack length are, in general, almost identically equal, however, the J_R curves based on the controlling condition of crack propagation is affectedby different ratio of biaxial loading and crack length. The unixial J_R curves (k=0) are higer than the biaxial J_R curves (k=0.5,1).

b. In comparsion, it is found that the modified Failure Assessment Diagram of EPRI method for biaxial loading proposed is more agreed with the experimental results than others.

c. Experimental and theorétical anlysis reveals that biaxially modified CEGB's R6 assessment method based on Dugdale's model gives a conservative prediction, and the biaxially modified Milne's assessment curve gives a good prediction.

It should be emphasised that all the experimental and theoretical analysis are based on biaxial cruciform specimen. Whether the results can be used in pressure vessels and piping needs further investigations.

REFERENCES

[1] Harrison R P, Loosemore K, Milne I, Dowling A R, Assessment of the integrity of structures containing defect, CEGB R/H/R6 -Rev 3 1980

[2] Shih C F, German M D and Kumar V. An engineering approach for examining crack growth and stability in flawed structures, Int. J. Press. Vess. and Piping, p, 1981

[3] Milne I, Failure Assessment Diagrams and J-Estimates: A Comparision for Ferritic and Austenitc Steel. Int. J. Press. Ves. and Piping, Vol.13, 1983

[4] Bloom J M. Procedure for the Assessment of the integrity of Nuclear Pressure Vessels and Piping Containing Defects. EPRI NP-2431, 1982

[5]. Miller K J and Kfouri A B. A Comparision of Elastic-Plastic Fracture Parameters in Biaxial Stress States. Elastic-Plastic Fracture, ASTM STP 668, 1979

[6] Alpa G, Bozzo E and Gamoarrotta L. Engineering Fracture Mechanics. EPRI Vol.12, 1979.

[7] Ming Yuan He and Hutchinson J N. Bounds for Fully Plastic Crack Problems for Infinite Bodies. ASTM STP 803, 1983